Journal of Nuclear Materials 442 (2013) 100–105

Contents lists available at ScienceDirect

Journal of Nuclear Materials

journal homepage: www.elsevier.com/locate/jnucmat

Novel high-strength ternary Zr–Al–Sn alloys with martensite structure for nuclear applications

Li Nie, Yongzhong Zhan *, Tong Hu, Xiaoxian Chen, Chenghui Wang

College of Materials Science and Engineering, Guangxi University, Nanning, Guangxi 530004, PR China

ARTICLE INFO

Article history:
Received 23 April 2013
Accepted 26 August 2013
Available online 31 August 2013

ABSTRACT

High strength is essential for the practical application of Zr alloys as structural materials. In this work, Zr–5Al–xSn ($x = 2$, 3, 4, 5 and 6) alloys have been designed and fabricated through arc melting in order to effectively improve the strength while retaining good ductility. Phase analysis results show that all the samples consist of single phase α-Zr. The variation trend of lattice constants as a function of Sn content has been analyzed. The microstructural analysis indicates that the Zr–5Al–xSn alloys mainly contain martensite structure. Mechanical tests show that these Zr–5Al–xSn alloys exhibit high compressive strength (1250–1450 MPa), high yield stress (800–1000 MPa), and favorable plastic strain of 18–23%. The fracture mode has been experimentally analyzed. Finally, both Zr–5Al–3Sn and Zr–5Al–5Sn are subjected to heat treatments for further study on the roles of Sn element and controlled heat treatment on the microstructure and mechanical properties of Zr alloys. Sn is found to promote the formation of ZrAl in the Zr–5Al–xSn alloys. Moreover, the martensite laths are observed to evolve into larger strip grains and fine equiaxed grains after heat treatment at 900 °C for 2 h. These factors strengthen the Zr–5Al–xSn alloys.

1. Introduction

Zirconium-based alloys are widely used in nuclear industry, mainly due to their small neutron absorption cross-section, favorable elevated-temperature mechanical properties, and excellent corrosion resistance, etc. [1–4]. The mechanical properties of iodide refining pure Zr are relatively low (for example, the ultimate strength is 180–270 MPa and the yield strength is 50–130 MPa [5]), which cannot afford to the standard of nuclear power used Zr alloys formulated by American Society for Testing Materials. That is, the strength of pure Zr should be remarkably improved to meet the requirement of nuclear industry.

At present, alloying method is the most common way for Zr-based alloys and two typical alloys i.e. Zr-2 and Zr-4 have been developed. The room-temperature ultimate strength of Zr-4 is up to 580 MPa, which is much higher than the pure Zr [5]. However, the mechanical properties of Zr alloys should be further improved to better satisfy the more and more complex conditions in nuclear industry. So far, in improving existing Zr alloys and developing new types of Zr alloys, the microstructure or chemical composition should be changed to obtain a good combination of mechanical properties and corrosion resistance.

As a common alloying element for Zr-based materials, Al can produce significant strengthening effect. It is typical alpha phase stabilizing element, so it is conducive to generate α-Zr at room temperature. For this reason, Zr–Al alloys have attracted the researchers' attention. For instance, metastable $Zr_{100-x}Al_x$ alloys have been prepared by ball milling of elemental Zr and Al powders, and supersaturated *hcp* solid solution was formed for $x \leqslant 15$, and an amorphous phase was formed for $x \geqslant 17.5$ [6]. The authors have found that Al element can refine the *in situ* ZrC particles in the Zr matrix composite, which has a compressive strength up to 1414 MPa [7]. In addition, 47Zr–45Ti–5Al–3V alloy with tensile strength higher than 1600 MPa has been developed, but the plasticity drops significantly [8].

Additionally, Sn element is often used in Zr alloys to increase the strength [9]. For instance, Lee et al. [10] have investigated the circumferential creep properties of stress-relieved Zircaloy-4 and found that the solution strengthening effect of Sn is more effective in restraining dislocation motion than the precipitate strengthening of Nb. By studying the creep and stress-rupture of high-strength Zr alloys, Ibrahim et al. [11] developed a Zr alloy (with composition of Zr–3 wt.%Sn–1 wt.%Mo–1 wt.%Nb) exhibiting high creep strength, low neutron capture cross-section and reasonable corrosion resistance.

To accelerate the industrial application of Zr-based materials, more fundamental researches are essential. In this work, we aim to effectively improve the strength and retain good ductility for Zr alloys. Al and Sn are used as alloying elements for this purpose. A series of Zr–5Al–xSn alloys with Sn content ranges from 2.0 to 6.0 at.% have been designed and prepared. Investigations on the

---

* Corresponding author. Tel.: +86 771 3272311; fax: +86 771 3233530.
E-mail address: zyzmatres@yahoo.com.cn (Y. Zhan).

0022-3115/$ - see front matter © 2013 Elsevier B.V. All rights reserved.
http://dx.doi.org/10.1016/j.jnucmat.2013.08.045

mechanical properties including compressive stress, yield stress and plastic strain in as-cast state have been performed. In addition, the phase composition and microstructure have been analyzed.

2. Experimental procedure

The Zr–5Al–*x*Sn alloys with nominal composition (in atomic fraction) of Zr–5Al–2Sn, Zr–5Al–3Sn, Zr–5Al–4Sn, Zr–5Al–5Sn and Zr–5Al–6Sn have been melted in the WK-II type non-consumable vacuum arc melting furnace. The raw materials were pure sponge zirconium (>99.9 wt.%), pure aluminum (>99.9 wt.%) and pure tin (>99.9 wt.%). In order to make the sample react and mix adequately in the molten state, the highest melting temperature was higher than 2000 °C by setting the current intensity. The reaction and melting time for each sample was kept for 80 s. The molten samples were cooled directly in the water-cooled copper melting pots (by running water at room-temperature). In order to ensure the chemical homogeneity of each sample, all ingots was turned over and remelted six times.

Samples for optical and secondary electron microscopy were cut by electric discharge machining (EDM) from the ingots. The samples for metallographic observations were mounted and mechanically polished with SiC paper and Al_2O_3 particles with water. The polished sample were etched in an erodent with composition of HF (aqueous solution): HNO_3 (aqueous solution): water = 1:2:6 (ratio by volume).

Phases identification were carried out via X-ray diffraction (XRD) using Rigaku D/Max 2500 V diffractometer with Cu Ka radiation and graphite monochromator operated at 40 kV and 200 mA. The microstructures were determined from DMM-660 type optical microscopy (OM) and Hitachi S-3400 N scanning electron microscope (SEM) equipped with energy dispersive (EDX) analysis. The dimension of the compression specimen was of 5 mm × 5 mm × 10 mm. Three samples were tested for each alloy to get the average values. Compression test was conducted at room temperature in air at an initial strain rate of 1 mm/min using the Instron 8801 axial servohydraulic dynamic testing system, to determine the mechanical properties like ultimate compressive strength, the fracture strain and plastic strain.

3. Results and discussions

3.1. Phase identifications and lattice constant analysis

Fig. 1 shows the XRD patterns of the as-cast Zr–5Al–*x*Sn ($x = 2$, 3, 4, 5 and 6) alloys. It is found that the solid state phase of all samples at room temperature is α-type Zr. According to the Zr–Al [12] and Zr–Sn [13] binary phase diagrams, the as-cast samples should also contain Zr_3Al and Zr_4Sn. However, it should be pointed out that these two phases may exist only when the temperature drops very slowly to provide enough time for the atomic diffusion to reach phase equilibria in the samples. However, the solid phase composition at room temperature is closely related to cooling rate after the alloys have solidified from high-temperature liquid. In this work, all the alloys were produced in the water-cooled copper crucible using arc melting. The cooling rate may be so fast for the small button samples that Zr_3Al and Zr_4Sn cannot be formed. In addition, Al and Sn are typical alpha phase stabilizing elements, which are conducive to generate α-Zr at room temperature. For example, in the Zr–Sn binary alloys, β phase can be quickly transformed into α phase. As a result, only α-Zr can be found in the as-cast samples. In addition, according to the Zr–Al and Zr–Sn binary phase diagrams, the present chemical components (Al and Sn) of the designed alloys have exceeded the maximum solid solubility of Zr, indicating that all these samples are supersaturated solid solution.

The variation of lattice constants, volume and density of the Zr–5Al–*x*Sn alloys as a function of Sn content has been discussed (as listed in Table 1). The α-Zr has hexagonal structure with space group P63/mmc (No. 194). As displayed in Fig. 2, only two Zr atoms exist in the unit cell, in which the 2c Wyckoff site (0.333, 0.667, 0.25) is occupied [14]. It is noted that the atomic radius of Zr is 2.16 Å, meaning that the voids of zirconium crystals is relatively large. The radii of Al and Sn atoms (1.82 Å and 1.72 Å, respectively) are much smaller than that of Zr atom, so they may form interstitial solid solution in the Zr matrix (the volume of unit cell may increase for forming an interstitial solid solution, while decrease for forming substitution solid solution). According to Table 1, it is found that the trends of lattice constants, volume exhibit nonlinear function with the Sn content. When Sn content is 4 at.%, the unit cell has the largest volume 46.62 $Å^3$. Moreover, we note that the trends of density of the Zr–5Al–*x*Sn alloys as a function of Sn content is also nonlinear, which should be related to the different rel-

Table 1
The lattice constants, volume of unit cell and density of the as-cast Zr–5Al–*x*Sn ($x = 2$, 3, 4, 5 and 6) alloys.

Alloys	*a* (Å)	*c* (Å)	*v* ($Å^3$)	*ρ* (g/cm^3)	Reference
Zr–5Al–2Sn	3.224	5.138	46.26	6.549	This work
Zr–5Al–3Sn	3.226	5.141	46.32	6.540	This work
Zr–5Al–4Sn	3.232	5.151	46.62	6.498	This work
Zr–5Al–5Sn	3.219	5.140	46.35	6.536	This work
Zr–5Al–6Sn	3.218	5.142	46.11	6.570	This work
Zr	3.232	5.147	46.57	6.500	[14]

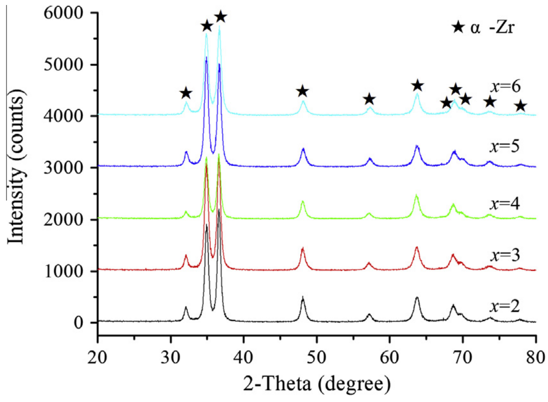

Fig. 1. XRD patterns of the as-cast Zr–5Al–*x*Sn ($x = 2$, 3, 4, 5 and 6) alloys.

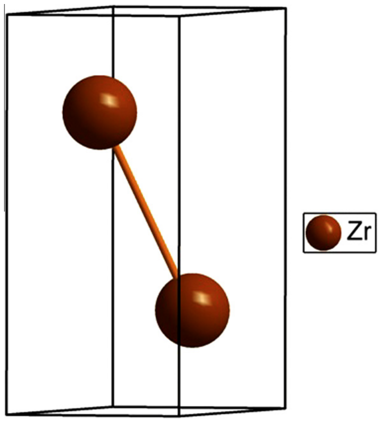

Fig. 2. The crystal structure of α-Zr.